Rheol Acta (2015) 54:353–364
DOI 10.1007/s00397-015-0845-z

ORIGINAL CONTRIBUTION

Two-step yielding in surfactant suspension pastes

Asheesh Shukla · Sumanth Arnipally · Manoj Dagaonkar · Yogesh M. Joshi

Received: 8 December 2014 / Revised: 16 February 2015 / Accepted: 22 February 2015 / Published online: 11 March 2015
© Springer-Verlag Berlin Heidelberg 2015

Abstract In this work, we investigate two-step yielding behavior of pastes containing anionic surfactants, clay, and abrasive particles of calcite. Such pastes are commercially used as hand dishwash paste. The surfactant suspension pastes have soft solid-like consistency with finite elastic modulus. The total volume fraction of the particulate matter in the same is around 36 %; consequently, we attribute the elastic modulus of the same to the bonding between abrasive particles leading to attractive gel phase. We observe that the surfactant suspension pastes undergo physical aging during which evolution of relaxation time takes place. In dynamic strain sweep experiments, the pastes demonstrate clear signature of two-step yielding. It is observed that during the first yielding event, elastic modulus decreases while viscous modulus shows a maximum. For the second yielding event, however, elastic modulus demonstrates plateau before decreasing. While the first yielding event is observed to remain unaffected by the frequency of oscillations, the plateau values of elastic modulus, before the second yielding process, is observed to increase with frequency. We attribute the first yielding event in surfactant suspension pastes to rupture of network, while the second yielding event to breakage of the aggregates.

Keywords Two-step yielding · Surfactant paste · Gel · Soft glassy materials

A. Shukla · Y. M. Joshi (✉)
Department of Chemical Engineering, Indian Institute of Technology Kanpur, Kanpur 208016, India
e-mail: joshi@iitk.ac.in

S. Arnipally · M. Dagaonkar
Unilever R&D Bangalore, 64, Main Road, Whitefield, Bangalore 560066, India

Introduction

Understanding how the rheological behavior is affected by the microstructure is crucial to effectively process the commercial soft materials to form saleable end products. Particularly for viscoelastic materials with complex microstructure that renders it extremely high viscosity, processing is a challenging task. Many commercial systems such as soaps, adhesives, hair gels, pharmaceutical and cosmetic creams, printing ink, etc., have soft solid-like consistency under ambient conditions. These systems contain a variety of ingredients including different kinds of surfactants, polymers, mixture of particles, and salts in aqueous or organic media. Moreover, the particles are not just present with different shapes and sizes but also with different surface functionalities. The presence of such ingredients leads to complex interactions among themselves, leading to a finite modulus. These materials also possess yield stress, a minimum stress that must be applied to induce flow. In this work, we study rheological behavior of surfactant-abrasive mixtures that are commercially used as hand dishwash pastes and incorporate a variety of interactions among its various constituents. Very interestingly, yielding in these materials is observed to occur in two steps. We analyze this behavior and relate the same to its microstructure.

It has been long debated in the literature whether yielding is a real phenomenon or merely an engineering manifestation wherein material undergoes a transition from weak flow to strong flow (Barnes 1999; Moller et al. 2009). The most recent literature, however, suggests that a section of the community indeed believes in existence of true yield stress, below which the materials absolutely do not flow (Moller et al. 2009). Usually the materials possess yield stress owing to significantly reduced mobility of its constituents. The primary reasons for such reduced mobility are either the crowding of constituents that arrest their neighbors to physical cages or sufficiently strong energetic interactions (van der Waals, electrostatic,

hydrogen bonding, hydrophobic, etc.) that immobilize the constituents so that they become a part of space spanning network. In some cases, both the aforementioned effects are simultaneously present (Joshi 2014). Irrespective of the nature of a microstructure, yielding event characterizes breakdown of the structure wherein constituents of the same gain mobility due to application of deformation field. Owing to complex inter-constituent interactions, some of these materials are out of thermodynamic equilibrium. Consequently, these materials undergo continuous structural organization to form progressively more stable microstructures. This process is known as physical aging (Cipelletti and Ramos 2005). Application of strong enough deformation field breaks the structures built during reorganization, a property known as rejuvenation or shear melting (McKenna et al. 2009). The behavior, wherein time-dependent evolution of physical properties can be reversed by application of deformation field, is known as thixotropy (Mewis and Wagner 2012). Yield stress associated with such materials is also time and deformation field dependent, and is termed as thixotropic yield stress (Moller et al. 2009). In some materials that undergo yielding, evolution of structure as a function of time is either absent or too slow over the practically achievable timescales. Yield stress in such materials is not time and deformation field dependent. This class of materials is called as simple yield stress materials. A huge amount of experimental and theoretical work has been reported in the literature on various aspects of yielding and on yield stress fluids in general. The details can be found out in a number of reviews published on this subject (Barnes 1999; Coussot 2014; Joshi 2014; Mewis and Wagner 2012; Moller et al. 2009; Vlassopoulos and Cloitre 2014).

There are various ways to experimentally determine the yield stress. One of the most prominent methods is to apply oscillatory flow field with increasing strain (or stress) magnitude (ramp) to a yield stress material. In the limit of small strain or stress, elastic (G') as well as viscous moduli (G'') remain constant with $G'>G''$. With the increase in stress, G' undergoes a significant decrease at the point of yield stress while G'' shows a maxima before decreasing. The magnitude of maximum, however, depends on frequency of the oscillatory flow field (Kamble et al. 2013). Recently, it has been reported that, rather than showing a single-step decrease in G', some soft materials show distinct two-step decay with the increase in the magnitude of oscillatory strain/stress. Since a sharp decrease in G' suggests breakdown of structure under the stress field, each decay in G' during yielding suggests the presence of structure over distinctly different length scales, which originates from diverse types of interactions. Pham et al. (2006) conducted experiments on sterically stabilized polymethylmethacrylate (PMMA) suspension in *cis*-decalin. In this suspension, PMMA particles interact via hard sphere interactions. However, incorporation of polystyrene, a non-adsorbing polymer, in the solvent introduces depletion attraction among the particles. Exclusion of polymer chains from the space in between the particles leads to osmotic pressure, which brings the particles further closer to each other, creating an "effective attraction" (Tadros 2005). Pham et al. (2006) observed that in the absence of attractive interactions, highly concentrated suspension showed only a single-step yielding. This yielding event was attributed to cage breakage due to enhanced mobility of particles upon application of strong deformation field. On the other hand, for attractive interactions among the particles in the presence of polystyrene (attractive glass), the material showed a distinct two-step yielding behavior. The authors attributed the first yielding event to the bond breaking process, while the second yielding was ascribed to breakage of cage. In a subsequent study, Pham et al. (2008) suggested that the amplitude of shear strain required for the bond breaking is proportional to the length scale associated with the inter-particle interactions. Since breaking of bonds releases the energy, a yielding event is accompanied by a peak in the loss modulus. Koumakis and Petekidis (2011) studied the same system of PMMA in *cis*-decalin. However, they varied the particle volume fraction while keeping the strength of depletion attraction same. The nature of the system varied from an attractive glassy phase at high volume fraction to attractive gel phase at low volume fraction. They reported the two-step yielding for both the phases, barring the systems at very low volume fraction. In both cases, the first yielding event was attributed to bond breaking. The second yield strain was attributed to cluster breaking for colloidal gels while cage breaking for attractive glasses. Shao et al. (2013) studied yielding behavior of aqueous carbopol microgel, wherein interactions undergo transition from repulsive to attractive with addition of salt (NaCl). Carbopol particles form a three-dimensional network structure in water, which they represent as microgel. It swells significantly at neutral pH. They observed that when interactions are repulsive, microgel undergoes yielding in only a single step. On the other hand, for predominantly attractive interactions, a two-step yielding is observed. In attractive gels, they attribute the first and the second yielding event to respectively the network and the cluster breaking. Zong et al. (2013) found two-step yielding in dense mixture of positively and negatively charged colloidal particles. Presence of two-step yielding has also been reported by Chan and Mohraz (2012) in dilute colloidal gel formed by sterically stabilized PMMA microspheres. They attributed the first yielding event to bond breakage, rotation, and gradual unwinding of the gel network structure. The second yielding was postulated to be associated with breaking of inter-particle bonds.

Two-step yielding is also observed in magneto-rheological systems by Segovia-Gutierrez et al. (2012). They used carbonyl iron particles suspended in silicone oil and observed two-step yielding in systems with high particle concentration and intermediate magnetic fields. However, only a single-step

yielding was reported in system with low concentration of particles. They proposed that yielding leads to formation of big clusters with strong intra-cluster bonds. At low concentration, the clusters do not interact with the other clusters, causing only a single-step yielding. At high concentrations, on the other hand, the clusters also form weak bonds with each other, which break at higher values of stress leading to the second yielding event. Koumakis and coworkers (Koumakis et al. 2013) observed two-step yielding in hard sphere colloidal glass. They used sterically stabilized PMMA hard spheres suspended in octadecene and octadecene-bromonapthalene mixture. They attributed yielding to interplay between Brownian motion and shear induced diffusion. The former dominates at low Peclet number, while the latter dominates at high Peclet number. Interestingly, for the intermediate Peclet numbers, where both the interactions superpose, two-step yielding with two peaks in G'' is observed. Sentjabrskaja et al. (2013) also reported two-step yielding in a binary suspension of hard spheres, which they attributed to the presence of two different length scales in the system. Interestingly, concentrated suspensions of anisotropic particles have also been reported to demonstrate two-step yielding (Kramb and Zukoski 2011). Overall, it is apparent that the two-step yielding has been observed in a wide variety of systems. However, a common thread running through these systems is the presence of at least two different types of interactions between the particles or more than one distinctly different characteristic length scales in the materials. The two-step yielding mechanisms for different systems discussed here have been summarized in Table 1.

In this work, we study yielding behavior of surfactant suspension pastes containing abrasive particles that are commercially used as hand dishwash pastes. It is well known that surfactants or amphiphilic molecules form various kinds of structures and mesophases in the liquid media including spherical or anisotropic micelles, wormlike micelles, lamellar phases, vesicles, and hexagonal phases (Israelachvili 2010). Occurrence of a particular mesophase depends upon temperature, nature of surfactants and solvent, their concentrations, salt, and presence of other ingredients that influence the interaction potentials (Larson 1999; Tadros 2005). A comprehensive discussion on various possible mesophases in surfactant solutions under various conditions is given elsewhere (Rosen 2004; Tadros 2005). However, generally speaking, at dilute concentrations, surfactants form largely an isotropic solution of spherically shaped micelles. Increase in concentration leads to micellar growth causing shape change from spherical to worm like. Addition of electrolyte also aids the formation of worm-like micelles (Tadros 2005). Further increase in concentration leads to formation of lyotropic liquid crystal phases with single or multiple phases coexisting together. At very high concentrations of surfactants, solution may undergo phase separation (Tadros 2005).

The rheology of surfactant solutions is strongly dependent on the nature of prevailing mesophase under given conditions. Surfactant solutions are known to demonstrate many interesting rheological features such as shear thinning, shear thickening (Richtering 2001), rheopexy and thixotropy (Mckeown et al. 2003), shear banding (Fielding 2014), etc. Application of deformation field is also observed to orient the mesophases, which in turn affects the rheological behavior. Richtering (2001) reported that lamellar phase in surfactant systems reorient themselves under applied shear. In some cases, on increasing shear rate, the lamellae flip to a perpendicular orientation and flip back to parallel alignment on further increase in shear rate (Berghausen et al. 1998). Lamellar phases have also been observed to form multilamellar vesicles (MLVs) on application of shear. The size of MLVs may depend on the shear rate.

Compared to literature on rheological and phase behavior of surfactant solution, the study of phase and rheological behavior of surfactant solutions containing particles has received significantly less attention. Interestingly, it has been recently reported that mesophases formed by surfactant can give rise to attraction among the suspended particles, through depletion interaction, leading to formation of gel (Buzzaccaro et al. 2007; James and Walz 2014; Petekidis et al. 2002). Petekedis et al. (2002) showed that in presence of worm-like micelles, formed by a mixed surfactant system, the charged polystyrene colloidal particles form a gel. The gels showed signs of aging with time, before collapsing under the effect of gravity. Buzzaccaro et al. (2007), who studied a surfactant depleted particulate system using light scattering experiments, found that for weak depletion, a colloidal system can be modeled by Baxter's "sticky" hard sphere model (Baxter 1968). For a strong depletion attraction, kinetically arrested gels are formed. They found that for the gel systems, storage modulus scales as power law of local concentration of particles. James and Walz (2014) studied the effect of ionic micelles on charged silica colloidal particles. They reported that above a critical concentration of surfactant, flocculation was observed in the system. The extent of flocculation was tunable, by controlling the depletion attraction induced in the system, which, in turn, can be controlled by controlling the surfactant concentration.

Materials, sample preparation, and experimental procedure

Materials and functions of various ingredients

The surfactant-abrasive paste used in this work consists of two types of surfactants, namely linear alkyl benzene sulfonates (LAS, procured from Rhodia Surfactants, India) and sodium lauryl ether sulfate (SLES, procured from Galaxy Surfactants,

Table 1 A brief survey of literature on two-step yielding

Paper	System used	Description	Fraction
Pham et al. 2006, 2008	Sterically stabilized PMMA particles, in *cis*-decalin. Depletion attraction induced by using PS	Hard sphere repulsive glasses and attractive glasses are formed. Two-step yielding is shown by attractive glasses, but not by repulsive glasses. First yielding attributed to breaking of attractive bonds, while second yield is attributed to cage breaking	ϕ=0.6
Koumakis and Petekidis 2011		Attractive colloidal gels and attractive colloidal glasses are formed. For ϕ <0.2, single-step yielding. For 0.2<ϕ<0.58, attractive gels are formed while for ϕ >0.58 attractive glasses are formed. As volume fraction is increased, the two-step yielding becomes more prominent. In glasses: bond breaking followed by cage breaking. In gels: bond breaking followed by cluster breaking	ϕ varied from 0.1 (gel) to 0.6 (glass)
Kramb and Zukoski 2011	Anisotropic particles of PS, stabilized by PEG suspended in 0.03 M NaCl solution	Hard colloidal glasses are formed. Two-step yielding is shown by heterodicolloid and symmetric homodicolloid shaped particles. Two steps attributed to two relaxation mechanisms by virtue of anisotropy in the particles. First yielding is attributed to particles rotating within the cage and second to particles' center of mass moving within the cage	ϕ: spherical=0.579 to 0.655. Heterodicolloid=0.588 to 0.678. Symmetric homodicolloid=0.638 to 0.704. Tricolloid=0.659 to 0.685
Chan and Mohraz 2012	Sterically stabilized PMMA particles, in mixed organic system. Depletion attraction induced by using PS	Depletion-induced dilute colloidal gels are formed. First yielding event is attributed to unwinding of gel network by bond rotation and rearrangements, and second is attributed to bond breaking	ϕ=0.05
Segovia-Gutiérrez et al. 2012	Carbonyl iron particle in silicone oil	Magneto-rheological fluids are studied. Two-step yielding is shown at intermediate magnetic fields (~10 kA) for ϕ >0.1. Mechanism is similar to that of attractive gels. First yielding is attributed to breaking of gel network into clusters. Second yielding is attributed to breaking clusters	Volume fractions=0.05 to 50 %
Koumakis et al. 2013	Sterically stabilized PMMA particles, in mixed organic system	Hard sphere glasses are formed. Two-step yielding is shown at intermediate Peclet number. At intermediate Peclet number, both Brownian motion aided yielding and shear induced diffusion act, resulting in two peaks in G''	ϕ=0.6 to 0.639
Sentjabrskaja et al. 2013	Sterically stabilized PMMA particles, in mixed organic system	Binary hard sphere mixtures, with size ratio up to 0.2, are formed. Two-step yielding has been linked with the presence of two equally dominant different length scales. Presence of two length scales leads to cages of different sizes. Although two length scales are present in all mixtures, in most samples, one dominates, thus leaving the second one less significant	ϕ=0.55 to 0.61
Shao et al. 2013	Aqueous carbopol microgel, with attraction induced by adding salt	Soft jammed repulsive glass and attractive colloidal gel are formed. As attractive strength is increased, the two-step yielding becomes more prominent. First yielding is attributed to network breaking followed by cluster formation. Second yielding is due to breaking of clusters	Weight %=0.5
Zong et al. 2013	Oppositely charged colloidal particles, with equal size and PS core and a thin PNIPAM shell, but have oppositely charged end groups. Mixed in equimolar ratio	Low volume fraction gel and high volume fraction glass are formed. Samples with ϕ <0.46 show one-step yielding, ϕ >0.46 show two-step yielding. The first yielding is linked to bond breakage between cages/clusters. The second yielding event is attributed to breaking of cages/clusters themselves. Cages appear in high volume fraction glasses, while clusters are found in low volume fraction gels	ϕ varied from 0.18 (gel) to 0.53 (glass).

PMMA polymethylmethacrylate, *PS* polystyrene, *PEG* polyethylene glycol, *PANIPAM N*-isopropyl acrylamide

India). LAS, an anionic surfactant, was neutralized using sodium hydroxide (procured from Sigma Aldrich LR) forming sodium linear alkyl benzene sulfonates (NaLAS). NaLAS, used in this work, is a multi-component mixture containing molecules having different alkyl chain lengths in the range C9 to C14. Furthermore, various isomers of the alkyl group with a given number of carbon atoms are also present in the surfactant; therefore, NaLAS does not necessarily contain only the linear alkyl groups. Furthermore, the industrial samples of LAS are known to have batch-to-batch variation in its composition with typical 10 % variation in alkyl chain configuration, variation in LAS content up to 2 %, and fluctuation in ionic components by around 0.2 to 0.3 % (Mckeown et al. 2003). In addition to surfactant, the paste also contains calcite (Saurashtra Chemicals, India), aluminosilicates, sodium carbonate, sodium hydroxide (all procured from Sigma Aldrich LR), kaolin clay (Dhirajlal and Co.), and water.

LAS is used as an acid precursor to the surfactant. Surfactants are added to the paste for a purpose of cleaning, lather generation, and binding of the paste matrix. SLES is also an anionic surfactant and produces hexagonal phase when mixed with water and increases the viscosity of the paste (Friedli 2001). Water, with these surfactants dispersed in the same, constitutes a viscous phase of the paste. These surfactants are known to form liquid crystalline phases in water, which also facilitates binding of the paste matrix. Calcite acts as abrasive and provides the scrubbing action during cleaning. The particle size of calcite is in the range 0.6–1905 μm. The volume weighted mean diameter ($D_{4,3} = \sum_i n_i d_i^4 / \sum_i n_i d_i^3$, where n_i is the number of particles having diameter d_i) is 87 μm. Furthermore, d (0.9) for the calcite particles is 122 μm. Here, d (0.9) is defined such that 90 % of the particles have diameter below d (0.9). Calcite is a mineral and primarily contains calcium carbonate ($CaCO_3$). It has specific gravity of 2.7 and Moh's hardness is 3 (Ciullo 1996). In Fig. 1a, SEM image of calcite is shown. The image is captured by AVEN Might Scope 5.0M Digital Microscope.

Sample preparation protocol

The process followed for making the paste was similar to what is reported in the literature (Aguilar et al. 2011; Choy and Argo 1994; Hartman 1977; Sathyanar et al. 2000). In a typical preparation procedure, LAS and SLES were added to an alkaline solution of demineralized water (made with addition of sodium carbonate and NaOH) taken in a beaker. The mixture was mixed for 5 min using an overhead stirrer at 50 rpm. To this mixture, calcite, aluminosilicates, and filler (kaolin clay) were added and mixed for 5 min. The process of mixing was carried out at 25 °C. The paste was then stored in an airtight container.

In this work, we studied the effect of abrasive, concentration of NaLAS, concentration of abrasive (calcite). The primary system studied in this work contains 14 wt.% surfactants (12 wt.% LAS and 2 wt.% SLES), 45 wt.% abrasives (calcite), 8 wt.% clay and other minor ingredients 7 wt.% (sodium carbonate and aluminosilicates), and remaining water. The sample containing 45 wt.% calcite is represented as A. We also studied different variants of samples by varying the composition and concentration of constituents, one component at a time. We also took SEM images of the dried paste samples using MIRA3 LM scanning electron microscope (TESCAN, Brno, Czech Republic). Prior to imaging, the samples were dried for 12 h at 150 °C and the dried powder was mounted on substrate. The corresponding image is shown in Fig. 1b. The image which is at much finer resolution clearly shows sharp edges of the abrasive particles.

Experimental procedure

Before beginning the experiments, a sample was taken out from the air-tight bottles and introduced in the shear cell carefully without any entrapped air bubbles. The experiments were conducted in a cup and bob geometry (bob diameter 10.004 mm with 0.407 mm gap) in Anton Paar Physica MCR 501 rheometer. After thermal equilibrium was attained at a desired temperature, the samples were pre-sheared by applying oscillatory strain of 3000 % at frequency=0.1 Hz for 10 min. Pre-shearing was carried out to eliminate any shear history. In this work, we carried out various tests such as time sweep (applying small amplitude oscillatory shear for a prolonged period of time to measure G' and G''), frequency sweep (at constant strain magnitude in the linear viscoelastic limit), and strain magnitude sweep. In the oscillatory experiments, G' and G'' were obtained by analyzing the response over six oscillations. Thus, the data represents steady-state values. While we performed all the experiments in the mentioned couette geometry having smooth walls, we also repeated some experiments with couette cell having serrated walls, particularly the strain sweep experiments. However, results with both the types of walls were observed to be practically identical within the experimental uncertainty, therefore ruling out a presence of wall slip.

Results

We first present the physical aging behavior of a sample A by applying small amplitude oscillatory shear for a prolonged period of time. In Fig. 2, the corresponding evolution of G' and G'' is plotted as a function of time at 25 °C. It can be seen that G' and G'' show a rapid increase at early times. However, beyond $t \approx 100$ s, G' practically remains constant. On the other hand, G'' shows a noticeable decrease as a function of time beyond $t \approx 100$ s. However, the decrease weakens with time and eventually reaches a plateau. In Fig. 3, frequency

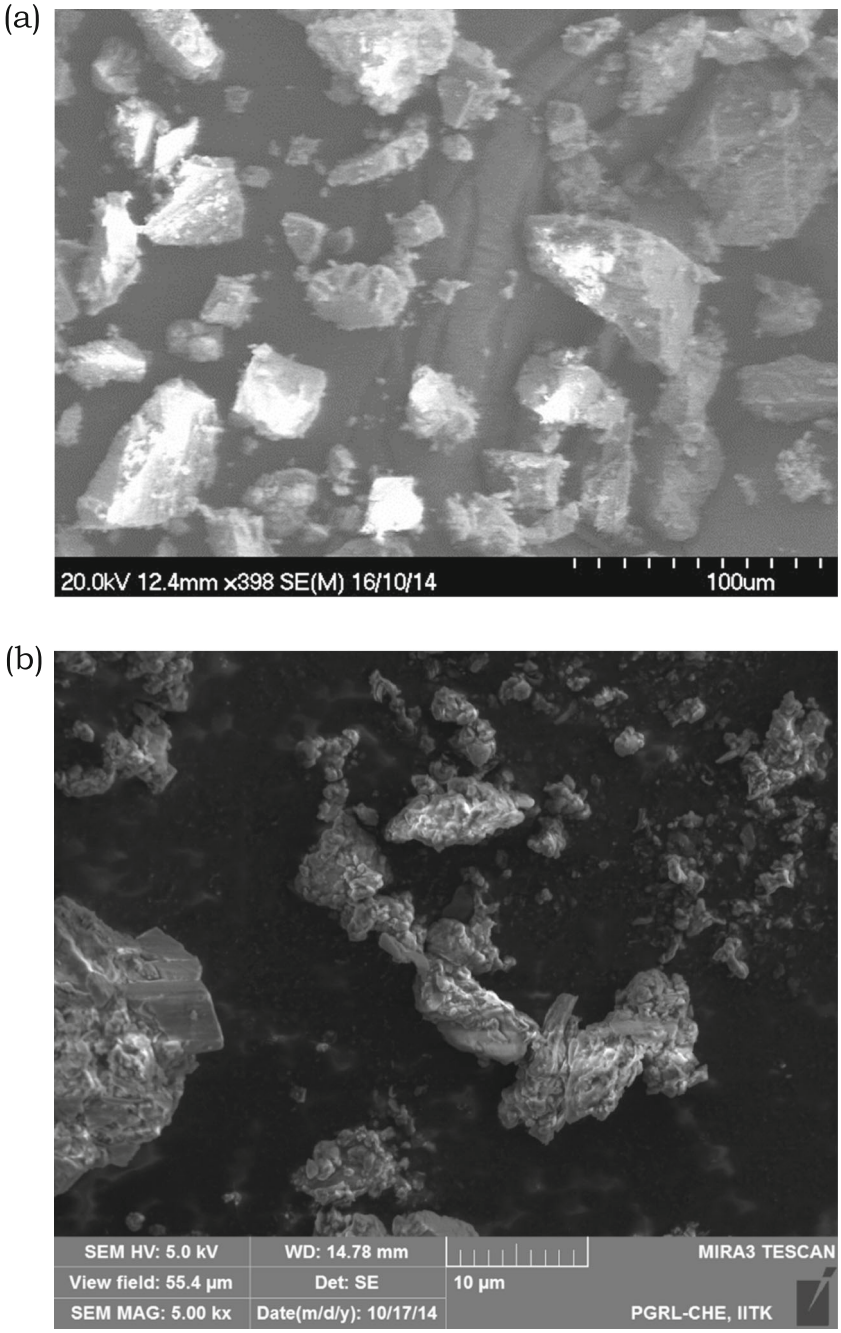

Fig. 1 **a** SEM image of abrasive particles of calcite. **b** SEM image of dried paste of sample A. In both cases, sharp edges of the particles can be clearly seen

dependence of G' and G'' immediately after the shear melting as well as subsequent to 8 h of aging at 25 °C is plotted for sample A. It can be seen that G' shows a weak increase as a function of frequency. Furthermore, curves associated with G' dependence on frequency before and after aging do not just follow the same trend but are quantitatively also very close to each other. Frequency dependence of G'' shows a prominent minimum, which shifts to lower values of frequency upon aging.

Next, we study the behavior of sample A under application of dynamic strain sweep. In Fig. 4, G' and G'' are plotted as a function of magnitude of strain at frequency ω=0.188 rad/s. It can be seen that, in the limit of very small strain, G' is observed to be greater than G''. In addition, in this limit, both the moduli are constant suggesting a linear viscoelastic limit. However, at certain critical strain, material yields causing a decrease in G'. During yielding, as observed for many soft materials, G'' shows a maximum before decreasing. Interestingly, G' decreases below G'' as the material yields and crosses over around the point where G'' shows a maximum. With the increase in strain magnitude, G' and G'' continue to decrease until a second critical strain is reached, where G' shows a

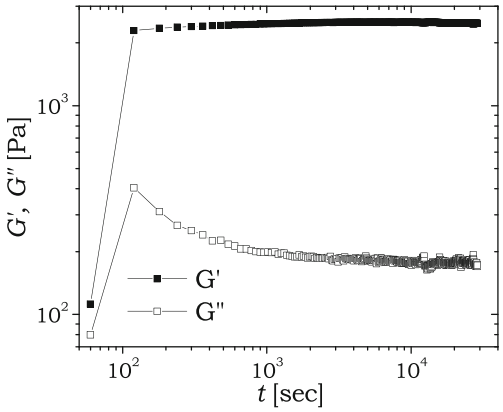

Fig. 2 Evolution of G' (*filled symbols*) and G'' (*open symbols*) during physical aging of sample A for 8 h at ω=0.628 rad/s and γ=0.1 %. It can be seen that beyond $t\approx$100 s, a gradual increase in G' can be observed

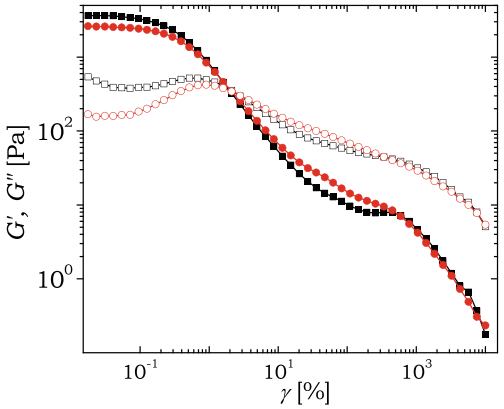

Fig. 4 Behavior of G' (*filled symbols*) and G'' (*open symbols*) is plotted as a function of magnitude of oscillatory strain in a dynamic strain sweep experiment carried out at ω=0.188 rad/s on sample A. The *symbols* are same as that in Fig. 3. It can be seen that aging does not have a noticeable effect on the yielding behavior of the sample

plateau before decreasing further at higher strains. In the vicinity of the second yield point, G'' also shows a noticeable shoulder before eventually decreasing at higher strains. Figure 4 therefore clearly shows a presence of two-step yielding in the surfactant suspension paste. In Fig. 4, we also plot the behavior of G' and G'' as a function of strain for 8 h aged sample. Interestingly, two-step yielding behavior of freshly shear melted and 8 h aged samples can be seen to be very similar to each other, suggesting aging does not have significant influence on the two-step yielding process. It should be noted that representation of material behavior in terms of G' and G'' is strictly restricted to linear regime wherein response is harmonic. While we did not obtain the complete stress waveform to the strain input, we did measure the ratio of the third harmonic in stress to the first harmonic in stress, in the dynamic strain sweep experiment. The mentioned ratio was always less than 0.1 throughout the experiment. Such behavior has been reported for a number of soft glassy materials, and since the waveform distortion is not significant, we represent the behavior in terms of G' and G'' (Koumakis et al. 2013; Krishnamoorti and Giannelis 2001; Shukla and Joshi 2009; Wyss et al. 2007).

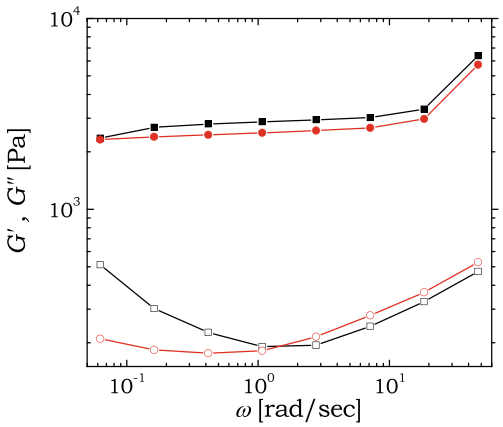

Fig. 3 Dependence of G' (*filled symbols*) and G'' (*open symbols*) on frequency at γ=0.1 % for sample A for the freshly shear melted samples (*squares*) and after aging for 8 h (*circles*)

In Fig. 5, we plot the yielding behavior of surfactant suspension paste at three different concentrations of calcite (variants of system A). In the main figure, G' and G'' are plotted as a function of strain while in the inset both the moduli are plotted as a function of magnitude of stress for the frequency of ω=0.031 rad/s. The sample of 45 wt.% calcite is the same as A. Interestingly, we observe that the two-step yielding behavior of 45 and 30 wt.% calcite pastes is similar except the second yielding behavior. We study the behavior of samples with calcite concentration lower than 25 wt.% as well. However, for concentrations $\leq$25 wt.%, abrasive particles are observed to undergo sedimentation over the duration of experiments due to higher density. Furthermore, we also study samples containing no abrasive particles but varying concentration of clay (system A contains 8 wt.% clay). We observe that for clay concentrations smaller than 6 wt.%, the paste is in a liquid state with $G'<G''$. Consequently, for 6 wt.% and lower concentrations of clay, paste becomes rapidly unstable due to significant sedimentation of clay particles. However, system of 8 wt.% clay concentration, without any abrasive particles, remains stable and does not show any sedimentation. Figure 5 shows yielding behavior of system containing 0 wt.% abrasive and 8 wt.% clay. It can be seen that at low strains (linear viscoelastic regime), G' is greater than G'', though the difference between both is not significant. Furthermore, with the increase in strain or stress, G' decreases and eventually crosses G'' thereby undergoing yielding. However, the sharpness of decrease can be seen to be significantly weaker than 30 and 45 wt.% calcite-containing samples. At higher strain or stress magnitudes, however, the sample with no abrasives demonstrates a clear G' plateau accompanied by a slight maximum in G'' before decreasing at further high strains.

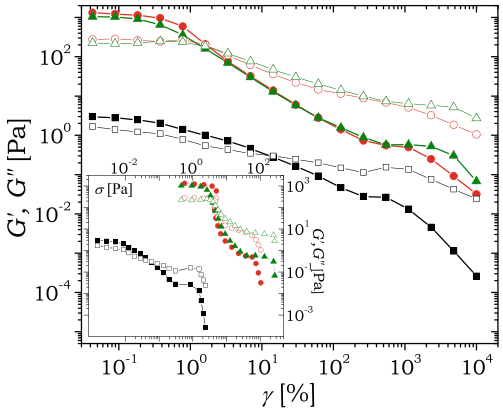

Fig. 5 Behavior of G' (*filled symbols*) and G'' (*open symbols*) is plotted as a function of magnitude of oscillatory strain at ω=0.031 rad/s for surfactant suspension pastes having 0 wt.% calcite (*squares*), 30 wt.% calcite (*circles*), and 45 wt.% calcite (*triangles*). Below the 25 wt.% concentrations of calcite, paste is observed to undergo sedimentation. The *inset* shows G' and G'' plotted as a function of magnitude of stress

We also study the effect of concentration of LAS on the rheological behavior of the surfactant suspension paste while keeping the concentration of SLES constant at 2 wt.%. As shown in Fig. 6, samples with different concentrations of LAS (with system having 12 wt.% LAS being same as A) demonstrate qualitatively similar two-step yielding behaviors with yielding curves shifting to higher modulus with the increase in concentration of LAS. It is known that LAS forms a lamellar phase in water over the explored concentrations (Stewart et al. 2009). It is therefore expected that greater concentration of lamella in water at higher concentration of LAS enhances rigidity of the continuous phase thereby increasing linear viscoelastic modulus of the paste.

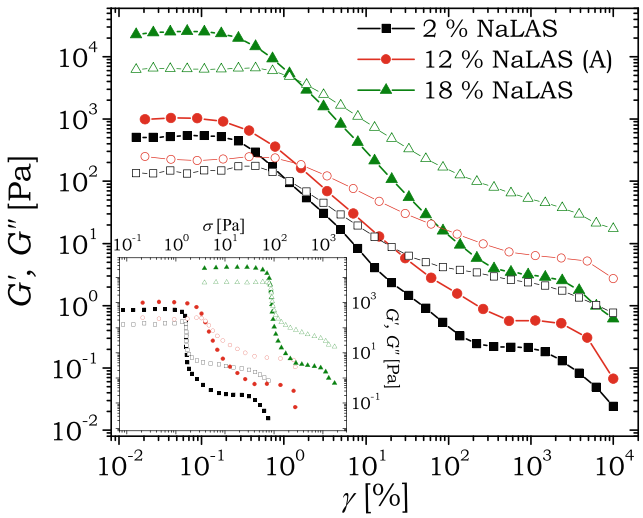

Fig. 6 Dependence of G' (*filled symbols*) and G'' (*open symbols*) on γ at ω=0.031 rad/s is plotted as a function of concentration of NaLAS. It can be seen that the increase in concentration of NaLAS shifts the curves to higher modulus without affecting the first and second yield strains. *Inset* shows the same data plotted as a function of magnitude of stress

In Fig. 7, the results of the oscillatory experiments on sample A as a function of amplitude of strain carried out at different frequencies are plotted. In Fig. 7a and b, respectively G' and G'' are plotted as a function of γ for different frequencies in the range 0.044 to 1.257 rad/s. In the insets of the same figures, the respective modulus as a function of σ are plotted. It can be seen that dependence of G' and G'' on γ as well as σ shows distinct variation with change in frequency. In the limit of small strains, G' and G'' follow linear viscoelastic behavior. With the increase in strain, material undergoes yielding. It can be seen that with variation in frequency, the yield stress and yield strain associated with the first yield point remain unchanged. Furthermore, during the first yield point, G'' shows a noticeable maximum irrespective of the frequency. The second yield point is characterized by a plateau-like region in G'. However, the plateau becomes progressively less intense with the increase in frequency. Before the second yield point, G'' also shows plateau at low frequencies. However, with the increase in frequency, plateau progressively changes to a gradual decrease as a function of strain. The characteristic behavior of G' and G'' is more apparent when plotted against stress as shown in the inset. It can be seen that plateau value in G'

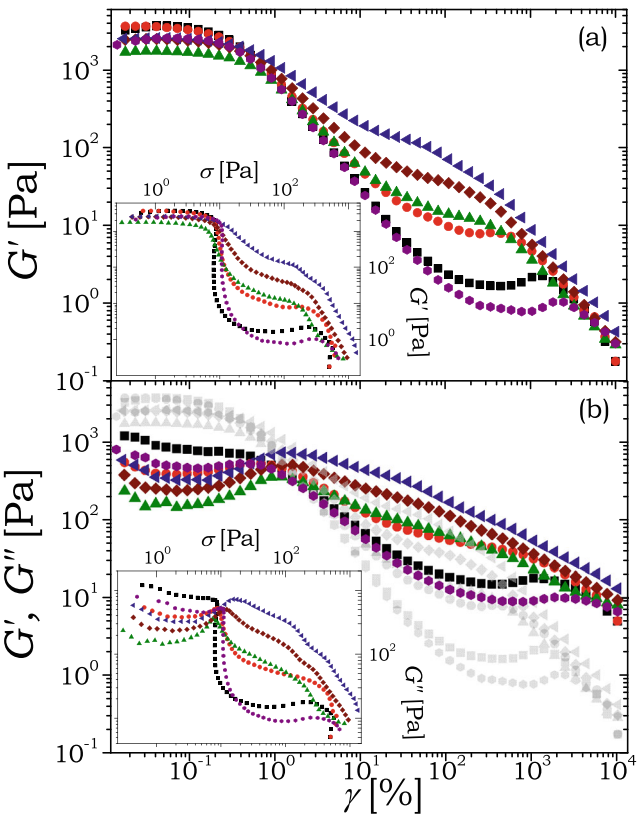

Fig. 7 Dependence of G' (*filled symbols*, **a**) and G'' (*open symbols*, **b**) on γ is plotted for different ω (in rad/s)=0.044 (*hexagon*), 0.063 (*square*), 0.188 (*circle*), 0.314 (*up triangle*), 0.628 (*diamond*), 1.257 (*left triangle*) for sample A. In the *inset*, both the moduli have been plotted as a function of magnitude of stress. It can be seen that with the decrease in frequency, both the yielding events become more prominent

associated with second yielding event increases with the increase in frequency. Unlike that observed during the first yielding event, G'' does not show any maximum during the second yielding event.

Discussion

We estimate the volume fraction of various ingredients by considering their weight fraction and density, which leads to volume fraction of abrasive particles having concentration of 45 wt.% to be 30.4 %. The material also contains 8 wt.% clay, which corresponds to a volume fraction of 5.9 %. We believe that a material cannot form attractive glassy state with a concentration of solid particles around 36 vol.%. Therefore, a material with volume fraction of solid particles as mentioned above can have significant modulus as shown in Figs. 2, 3, and 4 with $G'>G''$ in a linear regime only if the abrasive particles form a network (attractive gel) either completely by themselves or along with clay. It is well documented in the literature that various types of clays such as bentonite, kaolin, montmorillonite, and Laponite form an attractive gel at very small volume fractions (Luckham and Rossi 1999; Shahin and Joshi 2012; Van Olphen 1977). Therefore, it is very likely that clay particles along with abrasive particles form an attractive gel in surfactant suspension paste. Furthermore, as discussed in the "Introduction" section, clay and abrasive particles could also form an attractive gel through depletion interaction due to presence of surfactants in the solvent.

Figure 2 describes aging behavior of the system with calcite abrasive particles, wherein G' is observed to show very rapid increase over $t\approx100$ s followed by a constant value as a function of time. Interestingly, G'' also shows a rapid increase over the same duration; however, it is subsequently observed to show a noticeable decrease with time. It should be noted that during the shear melting step, a material, which is subjected to strong deformation field to remove any aging/shear history, is in the fluidized state. After stopping the shear melting, owing to enhanced mobility of the constituents, a material undergoes rapid structural reorganization, which causes a sharp increase in both the moduli over the observed period. According to Fielding and coworkers (Fielding et al. 2000), upon cessation of shear melting, constituents of soft glassy materials get arrested in energy wells whose depths are chosen randomly from the available distribution. Once the constituents are structurally arrested, their mobility gets significantly curbed. Under such situation, the constituents can only perform microscopic motions of structural rearrangement, which causes material to undergo physical aging. During this process, free energy of a material decreases with time. The physical aging in soft glassy materials is accompanied by enhancement in relaxation time as a function of time. The process of physical aging also, in principle, causes enhancement in elastic modulus. However, the increase in elastic modulus is often much weaker than that of relaxation time and in many cases not noticeable. If we approximate the present systems to obey single mode Maxwell model, viscous modulus of the same is given by $G''=G'/\omega\tau$, where ω is frequency of oscillations and τ is relaxation time. The decrease in G'', while G' almost remains constant, therefore suggests enhancement in relaxation time as a function of time in system A.

In Fig. 3, G' and G'' for the freshly prepared and 8 h aged sample A are plotted as a function of frequency. The system shows a weak increase in G' as a function of frequency. Interestingly, for system A, G'' shows a clear minimum that shifts to lower frequency upon aging. It should be noted that a weak increase in G' along with minimum in G'' as a function of frequency is known to be a distinctive characteristic feature of colloidal glassy (attractive as well as repulsive) materials. The time associated with inverse of frequency at which minimum in G'' occurs is considered to be related to transition from α timescale (cage diffusion) to β timescale (rattling motion inside a cage). Koumakis and Petekidis (2011) termed such timescale (inverse of frequency associated with minimum) to time related to exploration of the cage. For the systems studied in the present work, however, we believe that the microstructure is dominated by bonding between the abrasive as well as clay particles rather than caging. However, very recently, Jatav and Joshi (2014) reported a minimum in G'' when plotted against frequency for a significantly aged but shear melted colloidal gel of clay dispersion. They claimed that while shear melting of significantly aged colloidal gel breaks the network and induces fluidity, it cannot break every inter-particle bond leading to individual separate particles. Therefore, immediately after shear melting, paste contains solid pockets of unbroken network surrounded by fluidized paste. Such solid pockets can, in principle, act as cages to each other thereby demonstrating a minimum in G''. The present system, however, contains a variety of ingredients along with clay. Furthermore, the continuous phase contains surfactant mixture which itself is expected to show lamellar structure (Friedli 2001; Stewart et al. 2009). Therefore, it is difficult to speculate the exact mechanism that may lead to observed minimum in G'' in system A, though mechanism similar to that suggested by Jatav and Joshi (2014) cannot be ruled out.

In Fig. 5, the two-step yielding is analyzed as a function of concentration of abrasive particles. As mentioned before, paste with no abrasive particles and kaolin clay with concentration of 6 wt.% or less undergo sedimentation; however, paste with 8 % or more clay does not. Furthermore, paste having 8 wt.% clay and 25 wt.% or below abrasive particles also shows sedimentation of abrasive particles. Sedimentation is however not observed in paste with abrasives 30 wt.% and above. Interestingly, a similar behavior is also observed for dispersion of Laponite clay in water, wherein the dispersion is observed to undergo sedimentation below a critical

concentration, but is observed to form an attractive gel at higher concentrations (Mongondry et al. 2005). The sedimentation has been attributed to formation of weak gel at lower concentration which collapses under gravity (Mongondry et al. 2005). With the increase in concentration, however, strength of gel network increases and beyond a critical concentration gel is strong enough to sustain gravitational forces and demonstrates $G'>G''$ in the linear viscoelastic limit as observed experimentally.

For 0 wt.% abrasive and 8 wt.% clay system, the decay in G' as well as G'' is observed to occur over a broad range of magnitudes of strain (or stress). Such scenario is possible when network strands that connect the junctions in attractive gel break over a wide range of strains, which could arise from broad distribution of the lengths of the network strands. Interestingly, at higher concentration of abrasive particles (30 and 45 wt.%), the decay in G' and G'' is comparatively sharper and occurs at the smaller values of strain. As mentioned before, particles of calcite undergo sedimentation for concentrations of 25 wt.% and below. This suggests that at higher concentrations, calcite particles participate in the network formation independent of, or along with, clay particles. However, the network associated with the consequent attractive gel does not seem to be sufficiently flexible and breaks at lower values of strain compared to a system with no abrasive particles. Although the strain at the first yield point is small for 30 and 45 wt.% calcite concentration systems compared to 0 wt.% calcite concentration system, the stress associated with higher concentration calcite systems is higher. This is essentially due to greater modulus associated with the gel having higher concentration of calcite particles. Interestingly, Koumakis and Petekidis (2011), who studied the suspension of PMMA particles in *cis*-decalin, report that the strain associated with the first yielding event is divided in two regimes of volume fraction. In the higher volume fraction regime (>0.4), the first yield strain is independent of volume fraction with a value lower than that for low concentration suspension regime. For carbopol gels, Shao et al. (2013) observe the first yield strain decreases with increasing attraction.

In Fig. 6, we study the effect of concentration of LAS on the two-step yielding behavior. Interestingly, it can be seen that the strains at the first and the second yield point are independent of concentration of LAS, though G' and G'' shift to the higher values. The enhancement in G' and G'' may originate from three factors, namely, increase in network density, increase in inter-particle bond strength, and enhancement in elasticity of the continuous phase because of the increase in concentration of LAS. However, the increase in network density and strength will also cause change in the yield strains. The yield stress and G' can be related to yield strain as $\sigma_y \approx G'\gamma_y$. Interestingly, it is indeed observed that the factor by which yield stress and G' increases with the increase in concentration of LAS is identical within experimental uncertainty. Consequently, it appears that the concentration of LAS changes yield stress as it increases elasticity of the continuous phase; however, it does not affect yield strain as the network of particles possibly remains unaffected.

Similar to that suggested in the literature, the first yield point can be attributed to the rupture of network formed by clay and/or abrasive particles under application of stress. On the other hand, the second yielding event could originate from the breakage of aggregates of clay and abrasive particles. It can be seen from Fig. 5 that the strain associated with the second yield point increases with the increase in concentration of calcite. This suggests that with the increase in concentration of calcite, aggregates get deformed to progressively higher strains without breaking. Interestingly, for different concentrations of LAS, similar to the strain associated with the first yield point, the strain associated with the second yield point is also very similar. This indicates similar dynamics of aggregate breakage irrespective of the concentration of LAS. However, by virtue of different modulus, the stress associated with the second yield point is different. Literature suggests that the behavior of the strain associated with the second yield point is system specific because for attractive glass of PMMA particles, the second yield strain is observed to decrease with increasing volume fraction (Koumakis and Petekidis 2011). Interestingly Shao et al. (2013) observe that for carbopol gels, the second yield strain increases with the increase in attractive nature of the system.

In Fig. 7, we describe the frequency dependence of the two-step yielding behavior. It should be noted that at any specific magnitude of strain, the increase in frequency of oscillation essentially decreases the timescale of deformation (product of strain magnitude and frequency can be considered as magnitude of deformation rate). It can be seen that the strain and stress associated with the first yield point is independent of frequency. This suggests that the rupture of the network strands, which causes yielding, does not depend on the timescale of deformation field but is only a function of magnitude of strain. Consequently, the network breaks at certain strain, which causes a decrease in G' as well as G'' irrespective of the timescale of oscillations explored in this work. However, the rupture does not obliterate the network to individual particles thereby creating solid pockets containing unbroken aggregates that shear against each other in the fluidized paste. However, the fluidized paste also contains particles of abrasive mineral as well as clay, which are not part of the aggregates, along with surfactant in lamellar phase. The shearing of such paste between the solid pockets of aggregates is expected to induce significant stresses. Furthermore, owing to the roughness of particulate as well as aggregate surface as shown in Fig. 1, lack of hydrodynamic lubrication is not expected to prevent the particles from approaching each other leading to physical contacts (Zhao and Davis 2002). The resultant friction between the particles/aggregates may also contribute to

stresses (Seto et al. 2013). Magnitude of such stresses is expected to increase with the decrease in timescale of deformation field (increase in magnitude of deformation rate). Consequently, G' shows higher magnitude plateau with the increase in frequency for comparable magnitudes of applied strain. However, at further greater magnitudes of deformation rate, aggregates themselves break leading to the second yielding event. The curves shown in Fig. 7 are iso frequency curves, and with the increase in frequency, the second yielding event occurs at lesser strain. Importantly, the product of frequency and the value associated with the second yield strain is observed to be constant and in the range 80 to 100/s. Interestingly, this behavior is similar to that observed by Koumakis and Petekidis (2011) for suspension of PMMA particles in *cis*-decalin, wherein the first yield strain was observed to be independent of frequency for volume fractions in the range 0.4 to 0.6 and the second yield strain was observed to be decreasing with the increase in frequency. For attractive carbopol gels studied by Shao et al. (2013), on the other hand, both the yield strains are reported to be independent of frequency.

For a hand dishwash paste, the presence of two-step yielding has an important implication. When a cleaning scrubber is applied on hand dishwash paste, it must overcome stress associated with the first yield point. However, even though the first yield stress is crossed and paste is deformed to take it up on the scrubber, it does not lose its strength completely and starts flowing due to the presence of the second yielding point. In an optimum design, the range and separation of two yield stresses should be such that the typical application stress of a scrubber is in between the two limits.

Conclusion

In this work, we study two-step yielding of surfactant pastes that contain abrasive particles and clay, which are used commercially as hand dishwash pastes. Physical aging of this paste studied under application of oscillatory flow field suggests temporal evolution of relaxation time. The volume fraction of the abrasive particles in paste irrespective of their nature is about 30 %. The same associated with clay is around 6 %. Therefore, the particle volume fraction of around 36 % in the paste rules out a possibility of formation of glassy state (including attractive glass). The very fact that pastes show significantly high moduli with $G'>G''$ indicates the presence of network structure formed by both abrasive particles as well as clay.

In dynamic strain sweep experiments, the surfactant suspension pastes demonstrate clear signatures of two-step yielding. During the first yielding, G' decreases below G'' with the increase in strain. On the other hand, G'' shows a clear maximum during yielding. In all the samples studied in this work, both the moduli show a plateau before undergoing second yielding. Interestingly, the yield strains associated with both the yielding events have been observed to be independent of concentration of surfactant. Also, the first yielding event is observed to be independent of frequency. The plateau in G' just before the second yielding event, however, shifts to higher values of moduli with the increase in frequency. We believe that the first yielding phenomenon is associated with rupture of network. Breakage of network leads to formation of solid pockets of particle aggregates suspended in fluidized paste. The second yielding is believed to be related to breakage of such aggregates.

References

Aguilar J, Torres O, Chavez N, Alvarado M, Cazes A (2011) "Dishwashing paste" WO 2011 084780

Barnes H (1999) The yield stress—a review or 'panta roi'—everything flows? J Non-Newtonian Fluid Mech 81:133–178. doi:10.1016/S0377-0257(98)00094-9

Baxter RJ (1968) Percus–Yevick equation for hard spheres with surface adhesion. J Chem Phys 49:2770–2774. doi:10.1063/1.1670482

Berghausen J, Zipfel J, Lindner P, Richtering W (1998) Shear-induced orientations in a lyotropic defective lamellar phase. EPL (Europhys Lett) 43:683. doi:10.1209/epl/i1998-00417-3

Buzzaccaro S, Rusconi R, Piazza R (2007) "Sticky" hard spheres: equation of state, phase diagram, and metastable gels. Phys Rev Lett 99: 098301. doi:10.1103/PhysRevLett.99.098301

Chan HK, Mohraz A (2012) Two-step yielding and directional strain-induced strengthening in dilute colloidal gels. Phys Rev E 85: 041403. doi:10.1103/PhysRevE.85.041403

Choy CK, Argo BP (1994) "Thickening aqueous abrasive cleaner with improved colloidal stability", US patent 5279755

Cipelletti L, Ramos L (2005) Slow dynamics in glassy soft matter. J Phys Cond Mat 17:R253–R285

Ciullo PA (1996) Two—the industrial minerals. In: Ciullo PA (ed) Industrial minerals and their uses. William Andrew Publishing, Park Ridge, pp 17–82

Coussot P (2014) Yield stress fluid flows: a review of experimental data. J Non-Newtonian Fluid Mech 211:31–49. doi:10.1016/j.jnnfm.2014.05.006

Fielding SM (2014) Shear banding in soft glassy materials. Rep Prog Phys 77:102601. doi:10.1088/0034-4885/77/10/102601

Fielding SM, Sollich P, Cates ME (2000) Aging and rheology in soft materials. J Rheol 44:323–369. doi:10.1122/1.551088

Friedli F (2001) Detergency of specialty surfactants, vol surfactant science. CRC Press, 54–56

Hartman WL (1977) "Abrasive scouring compositions", US patent 4051056

Israelachvili JN (2010) Intermolecular and surface forces. Academic Press, London

James GK, Walz JY (2014) Experimental investigation of the effects of ionic micelles on colloidal stability. J Colloid Interf Sci 418:283–291. doi:10.1016/j.jcis.2013.12.015

Jatav S, Joshi YM (2014) Rheological signatures of gelation and effect of shear melting on aging colloidal suspension. J Rheol 58:1535–1554. doi:10.1122/1.4887344

Joshi YM (2014) Dynamics of colloidal glasses and gels. Ann Rev Chem Biomolecular Eng 5:181–202. doi:10.1146/annurev-chembioeng-060713-040230

Kamble S, Pandey A, Rastogi S, Lele A (2013) Ascertaining universal features of yielding of soft materials. Rheol Acta 52:859–865. doi:10.1007/s00397-013-0724-4

Koumakis N, Petekidis G (2011) Two step yielding in attractive colloids: transition from gels to attractive glasses. Soft Matter 7:2456–2470. doi:10.1039/c0sm00957a

Koumakis N, Brady JF, Petekidis G (2013) Complex oscillatory yielding of model hard-sphere glasses. Phys Rev Lett 110:178301. doi:10.1103/PhysRevLett.110.178301

Kramb RC, Zukoski CF (2011) Nonlinear rheology and yielding in dense suspensions of hard anisotropic colloids. J Rheol 55:1069–1084. doi:10.1122/1.3613978

Krishnamoorti R, Giannelis EP (2001) Strain hardening in model polymer brushes under shear. Langmuir 17:1448–1452. doi:10.1021/la0000365

Larson RG (1999) The structure and rheology of complex fluids. OUP, USA

Luckham PF, Rossi S (1999) Colloidal and rheological properties of bentonite suspensions. Adv Colloid Int Sci 82:43–92. doi:10.1016/S0001-8686(99)00005-6

McKenna GB, Narita T, Lequeux F (2009) Soft colloidal matter: a phenomenological comparison of the aging and mechanical responses with those of molecular glasses. J Rheol 53:489–516

Mckeown SA, Mackley MR, Moggridge GD (2003) Shear-induced structural changes in a commercial surfactant-based system. Chem Eng Res Des 81:649. doi:10.1205/026387603322150507

Mewis J, Wagner NJ (2012) Colloidal suspension rheology. Cambridge University Press, Cambridge

Moller P, Fall A, Chikkadi V, Derks D, Bonn D (2009) An attempt to categorize yield stress fluid behaviour. Philos Trans R Soc A Math Phys Eng Sci 367:5139–5155. doi:10.1098/rsta.2009.0194

Mongondry P, Tassin JF, Nicolai T (2005) Revised state diagram of Laponite dispersions. J Colloid Interface Sci 283:397–405

Petekidis G, Galloway LA, Egelhaaf SU, Cates ME, Poon WCK (2002) Mixtures of colloids and wormlike micelles: phase behavior and kinetics. Langmuir 18:4248–4257. doi:10.1021/la011751x

Pham KN, Petekidis G, Vlassopoulos D, Egelhaaf SU, Pusey PN, Poon WCK (2006) Yielding of colloidal glasses. Europhys Lett 75. doi:10.1209/epl/i2006-10156-y

Pham KN, Petekidis G, Vlassopoulos D, Egelhaaf SU, Poon WCK, Pusey PN (2008) Yielding behavior of repulsion- and attraction-dominated colloidal glasses. J Rheol 52:649–676. doi:10.1122/1.2838255

Richtering W (2001) Rheology and shear induced structures in surfactant solutions. Curr Opin Colloid Interface Sci 6:446–450. doi:10.1016/S1359-0294(01)00118-2

Rosen MJ (2004) Surfactants and interfacial phenomena. John Wiley & Sons, Inc Hoboken

Sathyanar MKV, Suresh R, Shivaji SD (2000) "Non-liquid abrasive composition", WO 2000020544

Segovia-Gutiérrez JP, Berli CLA, de Vicente J (2012) Nonlinear viscoelasticity and two-step yielding in magnetorheology: a colloidal gel approach to understand the effect of particle concentration. J Rheol 56:1429–1448. doi:10.1122/1.4742186

Sentjabrskaja T, Babaliari E, Hendricks J, Laurati M, Petekidis G, Egelhaaf SU (2013) Yielding of binary colloidal glasses. Soft Matter 9:4524–4533. doi:10.1039/c3sm27903k

Seto R, Mari R, Morris JF, Denn MM (2013) Discontinuous shear thickening of frictional hard-sphere suspensions. Phys Rev Lett 111:218301. doi:10.1103/PhysRevLett.111.218301

Shahin A, Joshi YM (2012) Physicochemical effects in aging aqueous laponite suspensions. Langmuir 28:15674–15686. doi:10.1021/la302544y

Shao Z, Negi AS, Osuji CO (2013) Role of interparticle attraction in the yielding response of microgel suspensions. Soft Matter 9:5492–5500. doi:10.1039/c3sm50209k

Shukla A, Joshi YM (2009) Ageing under oscillatory stress: role of energy barrier distribution in soft glassy materials. Chem Eng Sci 64:4668–4674. doi:10.1016/j.ces.2009.03.019

Stewart JA, Saiani A, Bayly A, Tiddy GJT (2009) The phase behaviour of lyotropic liquid crystals in linear alkylbenzene sulphonate (LAS) systems. Colloids Surf A Physicochem Eng Asp 338:155–161. doi:10.1016/j.colsurfa.2008.06.021

Tadros TF (2005) Applied surfactants. Wiley-VCH Verlag GmbH & Co. KGaA Weinheim

Van Olphen H (1977) An introduction to clay colloid chemistry. Wiley, New York

Vlassopoulos D, Cloitre M (2014) Tunable rheology of dense soft deformable colloids. Curr Opin Colloid Interface Sci. doi:10.1016/j.cocis.2014.09.007

Wyss HM, Miyazaki K, Mattsson J, Hu Z, Reichman DR, Weitz DA (2007) Strain-rate frequency superposition: a rheological probe of structural relaxation in soft materials. Phys Rev Lett 98:238303. doi:10.1103/PhysRevLett.98.238303

Zhao Y, Davis RH (2002) Interaction of two touching spheres in a viscous fluid. Chem Eng Sci 57:1997–2006. doi:10.1016/S0009-2509(02)00104-5

Zong Y, Yuan G, Zhao C, Han CC (2013) Differentiating bonding and caging in a charged colloid system through rheological measurements. J Chem Phys 138 doi:10.1063/1.4803857